Angular distributions and anisotropy of fission fragments from neutron-induced fission of ^{239}Pu, ^{237}Np, and ^{nat}Pb in energy range 1–200 MeV

A.S. Vorobyev[1,*], *A.M.* Gagarski[1], *O.A.* Shcherbakov[1], *L.A.* Vaishnene[1], *T.E.* Kuz'mina[2], and *A.L.* Barabanov[3,4]

[1]B.P. Konstantinov Petersburg Nuclear Physics Institute of NRC "Kurchatov Institute", Gatchina, Leningrad region, Russia
[2]V.G. Khlopin Radium Institute, Rosatom State Atomic Energy Corporation, St. Petersburg, Russia
[3]NRC "Kurchatov Institute", Moscow, Russia
[4]Moscow Institute of Physics and Technology, Dolgoprudny, Moscow Region, Russia

Abstract. This work summarizes some results of a series of experiments aimed at the investigation of energy dependence of anisotropy of fission fragments (FFs) in (n, f) reactions for neutron energies from low to intermediate. Angular distributions of FFs from the neutron-induced fission of ^{239}Pu, ^{237}Np, and ^{nat}Pb have been measured in the energy range 1–200 MeV at the neutron TOF spectrometer GNEIS based on the spallation neutron source at 1 GeV proton synchrocyclotron of the Petersburg Nuclear Physics Institute (Gatchina, Russia). The anisotropies of FFs deduced from the measured angular distributions are presented. In the neutron energy range above 20 MeV the results have been obtained for the first time in our works. The experimental data for FF anisotropy in ^{237}Np(n, f) are compared with calculations based on "adapted" TALYS software.

1 Introduction

The measurements of angular distributions of fission fragments (FFs) in neutron induced fission at relatively low (up to 20 MeV) and intermediate (up to 200 MeV) energies are of great interest for improving model concepts for mechanisms of neutron reactions. Indeed, the angular distributions of FFs depend not only on spectra of transition states on the barriers of fissioning isotopes, but on alignment of these isotope's spins too. But the spin alignment is much higher for the isotopes arising from the compound nucleus decay than for the isotopes formed after pre-equilibrium processes. Thus, the FF angular distributions provide important information on intensity of pre-equilibrium processes in neutron-nucleus interaction. Besides, the studies of highly excited nuclei decays are needed for the development of new technologies, such as the use of accelerator-driven systems (ADS) for nuclear power, nuclear waste transmutation, radiation testing of materials, nuclear medicine and other applications.

We began the study of the angular distributions of FFs in neutron induced fission of heavy nuclei at energies up to 200 MeV in 2014 at the neutron time-of-flight spectrometer GNEIS [1, 2] of the Petersburg Nuclear Physics Institute. At the previous ND-2016 conference we presented results for target nuclei ^{209}Bi, ^{232}Th, ^{233}U, ^{235}U, ^{238}U [3–5]. Currently, similar studies are also carried out by the n_TOF (CERN) [6, 7] and NIFFTE (LANSCE) [8] collaborations. This article focuses on our new measurements of the FF angular distributions in neutron-induced fission of ^{239}Pu, ^{nat}Pb and ^{237}Np in the energy range 1 – 200 MeV.

*e-mail: vorobyev_as@pnpi.nrcki.ru

2 Experiment and data processing

The measurements were performed at the 36-meter flight base of the spectrometer GNEIS. The detailed description of the experimental setup, the method of measuring the angular distributions of FFs and the procedures of the data analysis were given in our previous publications [3–5]. Here we will focus only on the most principal details and some important moments specific to this series of measurements.

The ^{239}Pu and ^{237}Np targets in the form of oxides were deposited by the "painting and baking" technique on an aluminum foil with a thickness of 100 μm. The active layer thicknesses was 300 μg/cm^2 and the diameters were 80 mm. The main isotope enrichment were 99.76% and 99.99% for ^{239}Pu and ^{237}Np, respectively. The ^{nat}Pb target with a thickness of 150 μg/cm^2 and a size of 120×120 mm^2 was made by vacuum deposition of high purity 99,9996% metallic Pb on a 2 μm thick Mylar foil.

The scheme of the experimental setup is shown in Fig. 1. The FFs were registered by two transparent position-sensitive low-pressure multi-wire proportional counters (MWPC) of 140×140 mm^2 size. Each of ones consisted of two anode (X,Y) and one cathode (C) wire electrodes. The detectors were located in the neutron beam one after another close to the fissile target. The axis of the neutron beam passed through the geometric centers of the MWPCs, being perpendicular to them. Signals from all electrodes were recorded using 500 MS/s waveform digitizer. Time and pulse height analysis of the recorded waveforms allows us to determine the neutron energy, coordinates of the FF registration on both detectors. Having the coordinates, it is possible to obtain the angle between

© The Authors, published by EDP Sciences. This is an open access article distributed under the terms of the Creative Commons Attribution License 4.0 (http://creativecommons.org/licenses/by/4.0/).

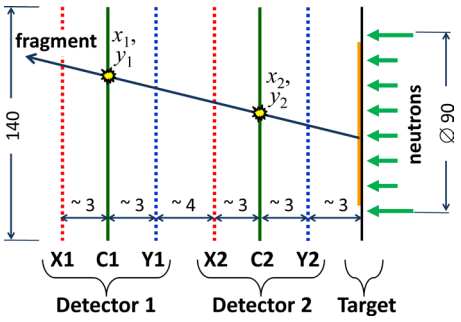

Figure 1. Scheme of the experimental setup (see text).

the FF momentum and the axis of the neutron beam. The neutron energy can be derived from time between neutron (gamma) flash and the cathode signals from FF detector. Thus, the angular distribution of FFs in the laboratory coordinate system (l.c.s.) was measured depending on the incident neutron energy.

The measured angular distributions were corrected to take into account the real geometry of the experiment, as well as the design and features of the MWPC (geometric efficiency, spatial resolution, etc.). The use of digital signal processing methods made it possible to measure the angular distributions of FFs in a wide energy range of incident neutrons with a practically zero registration threshold for FFs. An almost perfect separation of fission events from products of background reactions in constructing materials was achieved (see details in [4]). To obtain the angular distribution in the center-of-mass system (c.m.s.), it is necessary to take into account the momentum transferred to the nucleus by the incoming neutron. For this purpose, measurements of the angular distributions of FFs in the l.c.s. were carried out for two orientations of the installation relative to the direction of the neutron beam: the registered momentum of FFs is directed downstream and upstream of the neutron beam. The angular distribution in the c.m.s. was obtained by averaging of these two measured distributions in the l.c.s.

3 Results

We measured the angular distributions of FFs $W(\theta)$, where θ is the angle between the momentum of FFs and the neutron beam axis in the c.m.s., in the angular range $0.24<\cos(\theta)<1.0$ with a step of 0.01, as a function of the energy of incident neutrons in the range up to 200 MeV. Angular distributions for selected energy intervals can be approximated by expansion in even Legendre polynomials, it is sufficient to consider only polynomials of the 2nd and 4th order. In Fig. 2 taken from our work [9], the angular distributions of ^{239}Pu FFs for two neutron energies (~0.7 and ~14 MeV) are presented as an example in comparison with experimental data of other authors [10–13]. The fits of these distributions by the sum of even Legendre polynomials are shown in the same figure. For each neutron energy the anisotropy parameter was calculated as

$$\frac{W(0^\circ)}{W(90^\circ)} = \frac{1 + A_2 + A_4}{1 - A_2/2 + 3A_4/8}, \qquad (1)$$

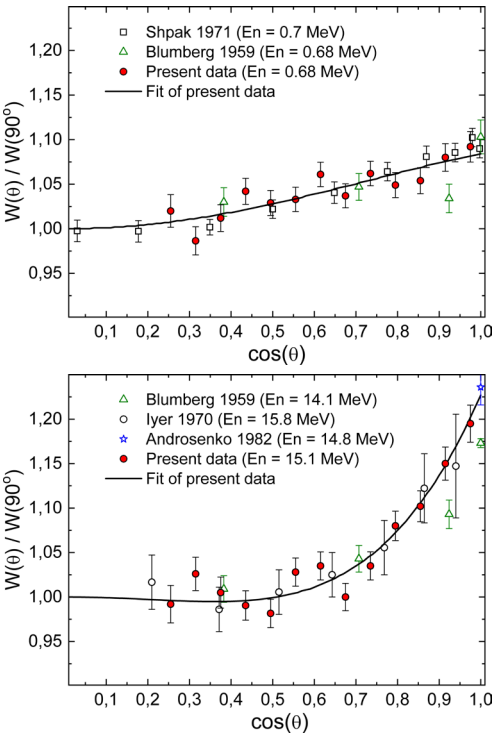

Figure 2. Angular distributions of FFs for ^{239}Pu for two characteristic energies of neutrons (~0.7 and ~14 MeV) compared with other EXFOR data [10–13]. Error bars are statistical errors. The solid lines are approximations of data by the sum of even Legendre polynomials up to the fourth order.

where A_2 and A_4 are coefficients of the 2nd and 4th order Legendre polynomials obtained by fitting procedure.

In Fig. 3 presented in [9], the anisotropy of FFs for ^{239}Pu and ^{nat}Pb obtained for the entire neutron energy range of 1–200 MeV is shown. The anisotropy for the fission of ^{237}Np was firstly published in [14] and reproduced in Fig. 4 here. The average error of our measurements for ^{239}Pu and ^{237}Np is 1-3%, and for ^{nat}Pb – 3-14% in the entire investigated neutron energy range. On the same figures for ^{239}Pu and ^{237}Np, the results of previous measurements of this anisotropy (^{239}Pu: [10–13, 15–18] and ^{237}Np: [12, 13, 15, 16, 19–21]) included in the EXFOR database are shown. Despite the fact that there are some differences between our data and the results of these earlier works, it can be said that there is generally a satisfactory agreement, especially if we take into account the existing discrepancy between the archival data sets. The data on the angular anisotropy of FFs from the neutron-induced fission of ^{239}Pu and ^{237}Np for energies above 16 MeV were obtained for the first time by our group. For a case of ^{nat}Pb fission shown in Fig. 3, there are also only our data. The estimating model calculation of Eismont et al. [22] performed for the isotope ^{208}Pb dominant in ^{nat}Pb is plotted in Fig. 3 for comparison. The parameters of this calculation were chosen to describe the data on the anisotropy of FFs in the ^{209}Bi(p, f) reaction. The discrepancy between our results for ^{nat}Pb and this model estimate may indicate a difference in the pre-equilibrium processes in reactions (n, f) and (p, f).

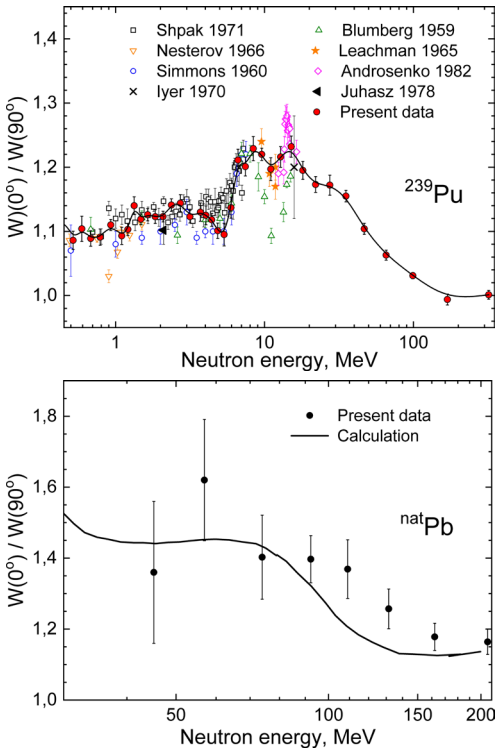

Figure 3. Anisotropy of FFs for ^{239}Pu (top) compared with experimental data from [10–13, 15–18] and for ^{nat}Pb (bottom). Error bars are the statistical errors. The solid line for ^{239}Pu is an eye guide to the experimental data. The solid line for ^{nat}Pb is the result of the model calculation [22].

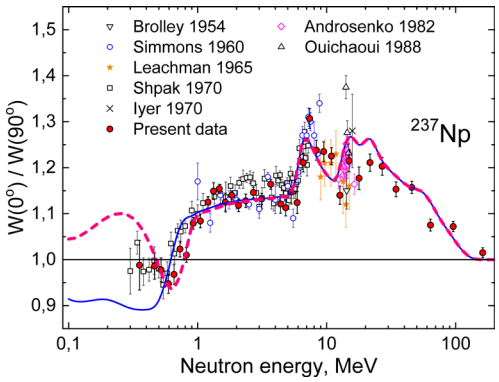

Figure 4. Anisotropy of FFs for ^{237}Np compared with old experimental data from [12, 13, 15, 16, 19–21]. Error bars are the statistical errors. The solid and dashed lines are the variants 1 and 2 of our model calculations, respectively (see text).

4 TALYS-based calculation for ^{237}Np

Besides the experimental results, we present a method for evaluation the FF angular distribution in neutron induced reactions at low and intermediate energies. The method is grounded on the same models for reaction mechanisms which are used in the TALYS software [23] for calculating total and partial cross sections. Therefore, based on TALYS, we compute differential fission cross section and, therefore, the FF angular distribution $W(\theta) = (d\sigma_f(\theta)/d\Omega)/\sigma_f$. We use the standard concept

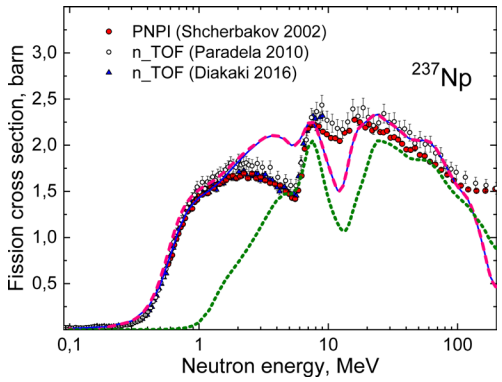

Figure 5. Fission cross section of ^{237}Np: experimental data [27–29], the dotted line is the calculation with default set of TALYS parameters, the solid and dashed lines are the variants 1 and 2 of calculations with adapted parameters, respectively (see text).

of transition states [24] and the corresponding equation $dw^J_{MK}(\theta)/d\Omega = (2J+1)|d^J_{MK}(\theta)|^2/4\pi$ for angular distribution of FFs of a fissioning nucleus with spin J and its projections K and M on the deformation axis and z axis, respectively.

At the 1st stage of neutron and target nucleus (Z_0, N_0) interaction, either the compound nucleus (Z_0, N_0+1) forms, or a fast particle and a residual nucleus (Z_1, N_1) arise in direct (D) or pre-equilibrium (PE) process. For simplicity, we neglect multiple pre-equilibrium processes and assume that each residual nucleus (Z_1, N_1) undergoes a sequence of statistical decays just like the compound-nucleus (Z_0, N_0+1). Any nucleus (Z, N), formed at the 1st stage of the reaction or at some stage of statistical decay, can divide into two fragments. Let the index i numbers the levels of the nucleus (Z, N) with the same spin J and parity π. Let $\sigma_{ZNJ\pi i}(M)$ be the population cross section for the state (J, π, i) of the nucleus (Z, N), where M is the projection of J on the axis z, while $\sigma^C_{ZNJ\pi i}(M)$ and $\sigma^{DPE}_{ZNJ\pi i}(M)$ are its components. They originate from compound nucleus and residual nuclei (Z_1, N_1) decays, respectively. If spins s and I of colliding particles are non-oriented, then the spin $\mathbf{J} = \mathbf{s} + \mathbf{I} + \mathbf{l}$ is directed mainly transversely to the collision axis (axis z) due to the orbital momentum l. Therefore, the distribution of the compound nucleus states over M is very non-uniform or, in other words, the compound states are aligned. This alignment is transferred to the residual nuclei, so that the cross sections $\sigma^C_{ZNJ\pi i}(M)$ have noticeable non-uniformity in M. But it is not the case for the cross sections $\sigma^{DPE}_{Z_1N_1J\pi i}(M)$ and, therefore, for the associated population cross sections for residual nuclei. To simplify, we assume that the *DPE* contribution to the differential fission cross section is isotropic. Thus $d\sigma_f(\theta)/d\Omega = \sigma^{DPE}_f/4\pi + d\sigma^C_f(\theta)/d\Omega$, and

$$\frac{d\sigma^C_f(\theta)}{d\Omega} = \sum_{ZNJ\pi iM} \sigma^C_{ZNJ\pi i}(M)\, P^{J\pi i}_{fZN} \sum_K \rho^{J\pi i}_{ZN}(K)\, \frac{dw^J_{MK}(\theta)}{d\Omega}, \tag{2}$$

where $P^{J\pi i}_{fZN}$ is the fission probability, and $\rho^{J\pi i}_{ZN}(K)$ is its distribution over K. Earlier, a model based on similar principles was used in [25] to evaluate the FF angular anisotropy

for neutron induced fission of even-even nuclei ^{232}Th and ^{238}U at energies 2 – 100 MeV, however, no publications on other nuclei followed. Moreover, there are no other publications on the calculations of the FF angular distributions for intermediate-energy neutrons. In practice, instead the formula (2) we use the result of its transformation to a series in terms of Legendre polynomials (see details in [14]). For the distribution of the fission probability over K we use the statistical approach $\rho^{J\pi i}_{ZN}(K) \sim e^{-K^2/2K_0^2}$ at high excitation energy [24], while at low one we assume that fission occurs predominantly through a transition state with a projection K_1: $\rho^{J\pi i}_{ZN}(K) \sim e^{-\alpha(|K|-K_1)^2}$.

As a test of the method we reproduce the data obtained for ^{237}Np, using a minimal set of parameters besides those embeded to the TALYS. Notice, however, that the ^{237}Np(n, f) reaction cross section, calculated by TALYS with default parameters [26] and explicit account of collective enhancement for the level densities, strongly differs from the results [27–29] – see Fig. 5 (formerly presented in [14]). Adjusting parameters of transition states and barriers (but without changing the level density) for $^{238-236}$Np, we obtained the fission cross section, which, up to 100 MeV, reasonably agrees with the measured one (variants 1 and 2 in Fig. 5 differ in transition states for ^{238}Np, but almost identically describe the cross section). Then calculating the differential fission cross section and using 5-6 additional parameters to describe K-dependence of the fission probabilities (see details in [14]), we obtained a good description for the gross structure of the observed angular anisotropy – see Fig. 4, where K_1 for ^{238}Np is equal to 0 and 4 for the variants 1 and 2, respectively (all intermediate values for K_1 "push" the anisotropy observed at 0.5–0.6 MeV to the region of values exceeding 1). This result demonstrates the validity of our TALYS-based model and allows to relate the decrease of FF angular anisotropy with the energy growth above 20–30 MeV to an enhancement of the pre-equilibrium processes.

5 Summary

The measured FF angular distributions are presented for (n, f) reactions at ^{239}Pu, ^{237}Np and ^{nat}Pb nuclei at 1–200 MeV. Our data agree with those available in the literature for energies below 16 MeV. For energies above 16 MeV our data are unique. The TALYS-based calculation of FF angular anisotropy for the ^{237}Np(n, f) reaction is demonstrated. The results for energies up to 200 MeV are consistent with the experimental ones. Further development of theoretical description of nuclear dynamics at low and high excitation energies and its use for experimental data analysis would provide important information on both the fission process and the reactions at intermediate energies.

The authors express their thanks to the staff of the Accelerator Department of the PNPI for the support and smooth operation of the neutron source. Partial support from the RFBR (Russia) – Grant No.18-02-00571 is greatly acknowledged.

References

[1] N.K. Abrosimov et al., Nucl. Instrum. Methods Phys. Res. A **242**, 121 (1985)
[2] O.A. Shcherbakov et al., Phys. Part. Nucl. **49**, 81 (2018)
[3] A.S. Vorobyev et al., JETP Lett. **102**, 203 (2015), EXFOR entry #41608
[4] A.S. Vorobyev et al., JETP Lett. **104**, 365 (2016), EXFOR entry #41616
[5] A.S. Vorobyev et al., EPJ Web Conf. **146**, 04011 (2017)
[6] D. Tarrío et al., Nucl. Data Sheets **119**, 35 (2014), EXFOR entry #23209
[7] E. Leal-Cidoncha et al., EPJ Web Conf. **111**, 10002 (2016)
[8] V. Geppert-Kleinrath et al., Phys. Rev. C **99**, 064619 (2019)
[9] A.S. Vorobyev et al., JETP Lett. **107(9)**, 521 (2018), EXFOR entry #41658
[10] L. Blumberg, R.B. Leachman, Phys. Rev. **116**, 102 (1959), EXFOR entry #13710003
[11] D.L. Shpak et al., Sov. J. Nucl. Phys. **13**, 547 (1971), EXFOR entry #40124003
[12] R.H. Iyer, M.L. Sagu, *Proc. Nucl. and Solid State Phys. Symp., Vol. 2* (Madurai, 1970) 57, EXFOR entry #30235
[13] Kh.D. Androsenko et al., VANT, Ser. Yad. Konst. (in Russian) **2/46**, 9 (1982), EXFOR entry #40825
[14] A.S. Vorobyev et al., JETP Lett. **110(4)**, 242 (2019)
[15] J.E. Simmons, R.L. Henkel, Phys. Rev. **120**, 198 (1960), EXFOR entry #13706
[16] R.B. Leachman, L. Blumberg, Phys. Rev. **137**, B814 (1965), EXFOR entry #13708
[17] V.G. Nesterov et al., Sov. J. Nucl. Phys. **4**, 713 (1967), EXFOR entry #40366004
[18] S. Juhasz, M. Varnagy, *Zentralinst. f. Kernforschung Rossendorf Reports, No. 376* (1978) 135, EXFOR entry #30510
[19] J.E. Brolley, W.C. Dickinson, Phys. Rev. **94**, 640 (1954), EXFOR entry #13707005
[20] D.L. Shpak et al., Sov. J. Nucl. Phys. **12**, 19 (1971), EXFOR entry #40277002
[21] S. Ouichaoui et al., Acta Physica Hungarica **64**, 209 (1988), EXFOR entry #30819007
[22] V.P. Eysmont et al., AIP Conf. Proc. **769**, 633 (2005)
[23] A.J. Koning et al., *Proc. Int. Conf. on Nucl. Data for Science and Technology* (EDP Sciences, 2008) 211
[24] R. Vandenbosch, J.R. Huizenga, *Nuclear Fission* (Academic Press, New York, 1973)
[25] I.V. Ryzhov et al., Nucl. Phys. A **760**, 19 (2005)
[26] R. Capote et al., Nucl. Data Sheets **110**, 3107 (2009)
[27] O. Shcherbakov et al., J. Nucl. Sci. Tech. **39 (suppl. 2)**, 230 (2002), EXFOR entry #41455011
[28] C. Paradela et al., Phys. Rev. C **82**, 034601 (2010), EXFOR entry #23126003
[29] M. Diakaki et al., Phys. Rev. C **93**, 034614 (2016), EXFOR entry #22742004